View metadata, citation and similar papers at core.ac.uk

brought to you by CORE

provided by Elsevier - Publisher Connector

Available online at www.sciencedirect.com

ScienceDirect

Polar Science 2 (2008) 267–276

http://ees.elsevier.com/polar/

# Interpretation of the GRACE-derived mass trend in Enderby Land, Antarctica

Keiko Yamamoto [a,*], Yoichi Fukuda [a], Koichiro Doi [b], Hideaki Motoyama [b]

[a] *Department of Geophysics, Graduate School of Science, Kyoto University, Kyoto, Japan*
[b] *National Institute of Polar Research, Tokyo, Japan*

Received 7 January 2008; revised 27 September 2008; accepted 9 October 2008
Available online 6 November 2008

**Abstract**

Monthly gravity solutions of the Gravity Recovery and Climate Experiment (GRACE) reveal three areas in Antarctica with striking interannual mass trends. The positive mass trend in Enderby Land, East Antarctica, is poorly understood because of uncertainties in the surface ice-sheet mass balance, post-glacial rebound (PGR), and processing of GRACE data. In this study, we compare the GRACE mass trends with values estimated from *in situ* snow-stake measurements, and Ice Cloud and land Elevation Satellite (ICESat) data. The mass trends estimated from ICESat data show a strong correlation with GRACE mass trends. In contrast, the snow-stake data show discrepancies with temporal variations in GRACE mass, especially in 2006. The discrepancies are probably associated with basal ice-sheet outflow, which is difficult to observe using snow stakes. We conclude that the bulk of the GRACE mass trend can be explained by snow accumulation and basal ice-sheet outflow.
© 2008 Elsevier B.V. and NIPR. All rights reserved.

*Keywords:* Antarctic ice-sheet mass balance; GRACE; ICESat; Snow-stake measurements

## 1. Introduction

The Antarctic ice sheet holds about 90% of the world's ice, representing about +60 m of global sea-level change. Therefore, a small change in the Antarctic ice-sheet mass could have a significant effect on global sea-level (Church et al., 2001). Given that accurate knowledge of the ice-sheet mass balance in Antarctica is an important factor in studies of global climate change, many research efforts have addressed this subject (e.g., Davis et al., 2005; Rignot and Thomas, 2002). Ice-sheet mass balance is generally estimated using the mass budget method, which calculates the net accumulation minus loss for each of many small regions; however, it is difficult to determine large-scale ice-sheet mass balance following this method because of large uncertainties in estimating accumulations and losses; reliable results are obtained for small regions when GPS and Interferometric Synthetic Aperture Radar (InSAR) data are employed.

Satellite and airborne altimetry provide information on ice sheet changes based on measurements of elevation changes over time; however, the effects of compaction and snow density (which are required to convert elevation change to mass balance) are poorly constrained over large areas. Thus, before the launch of the Gravity Recovery and Climate Experiment

* Corresponding author. Research Institute for Humanity and Nature, 457-4, Motoyama, Kamigamo, Kita-ku, Kyoto 603-8047, Japan.
*E-mail address:* yamamoto@chikyu.ac.jp (K. Yamamoto).

1873-9652/$ - see front matter © 2008 Elsevier B.V. and NIPR. All rights reserved.
doi:10.1016/j.polar.2008.10.001

(GRACE) satellite in 2002 (Tapley et al., 2004), estimates of Antarctic ice-sheet mass balance yielded unsatisfactory results, especially over large areas. GRACE has provided information on temporal mass variations on Earth in the form of monthly gravity-field solutions, and has enabled the direct monitoring of ice-sheet mass changes. In particular, GRACE can reveal total mass variations in Antarctica (Velicogna and Wahr, 2006), which are closely related to global sea-level change; however, GRACE cannot distinguish between the various sources of mass variations.

It is well known that post-glacial rebound (PGR) leads to pronounced mass trends in Antarctica. Velicogna and Wahr (2006) estimated the interannual ice-sheet mass trend by subtracting the PGR mass trend using the ice models IJ05 (Ivins and James, 2005) and ICE-5G (Peltier, 2004). Chen et al. (2006) calculated spatial variations in the Antarctic mass trend by subtracting the PGR influence using the IJ05 ice model, and determined two prominent mass trends in West and East Antarctica.

As shown in Fig. 1(a), three areas with striking interannual mass trends are commonly observed by GRACE data: 1) a positive trend around the Antarctic Peninsula and Filchner and Ronne Ice Shelves (AP/FRIS), 2) a negative trend around Pine Island Glacier (PIG), and 3) a positive trend in Enderby Land (EL), East Antarctica (50−60° E). Among these mass trends, the large positive trend over EL remains poorly explained. Chen et al. (2006) argued that this trend is inconsistent with recent estimates of the surface mass rate and the latest ice model. The authors suggested that the source of the trend may be unquantified snow accumulation or, more likely, unmodeled PGR.

In the present study, we focus on the sources of the positive regional mass trend observed in EL. We compare GRACE results with PGR models, Ice Cloud and land Elevation Satellite (ICESat) laser altimeter data (Zwally et al., 2002), and snow-stake data collected by the Japanese Antarctic Research Expedition (JARE), and investigate the possible sources of the mass trend observed in the region.

## 2. Data processing

### 2.1. GRACE data and processing

We analyzed the GRACE Level-2 monthly gravity-field solutions provided by the Center for Space Research, University of Texas, USA Release 4 (UTCSR RL04) (Bettadpur, 2007) for the period from April 2002 to June 2007. For comparison, we also used other versions of GRACE Level-2 solutions: the Jet Propulsion Laboratory Release 4 (JPL RL04) (Watkins, 2007) and GeoForshungsZentrum Release 4 (GFZ RL04) (Flechtner, 2007). The $C_{20}$ components were replaced with those from Satellite Laser Ranging (SLR) solutions (Cheng and Ries, 2007).

To demonstrate the general features of the spatial distribution of the interannual mass trends, we first

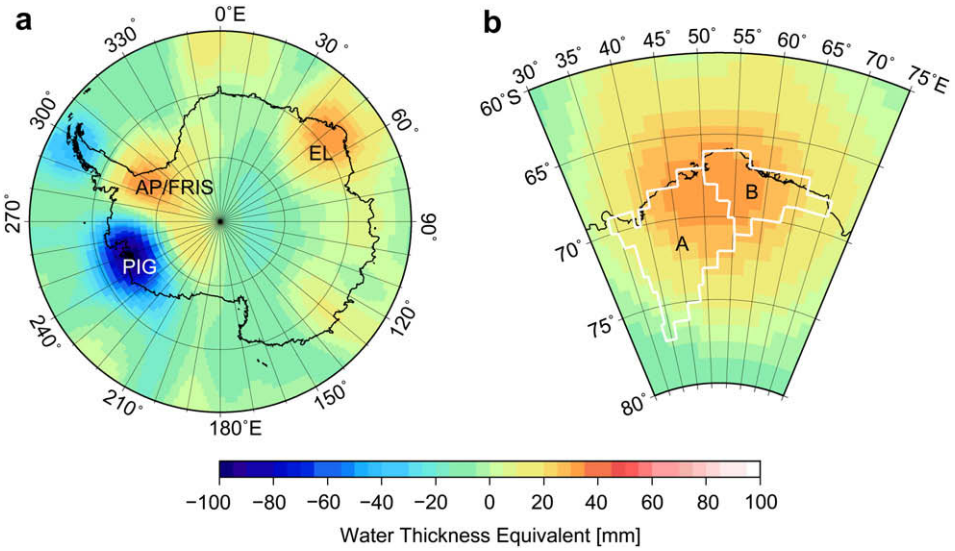


Fig. 1. (a) Interannual mass trend in Antarctica estimated based on GRACE data with a 500 km filter. AP/FRIS shows the Antarctic Peninsula and Filchner and Ronne Ice Shelves. PIG and EL shows Pine Island Glacier and Enderby Land, respectively. (b) Mass trend in Enderby Land. A and B are the basins analyzed in this study.

applied a globally normalized Gaussian filter with a 500 km correlation length (Wahr et al., 1998). Fig. 1(a) shows the filtered mass trend of the UTCSR RL04 solution. JPL RL04 and GFZ RL04 solutions show similar spatial patterns (data not shown). The three areas with prominent trends (AP/FRIS, PIG, and EL) are commonly observed in these results, although the PIG and AP/FRIS trends are not discussed in this paper.

For a precise evaluation of the signal amplitude of EL, we designed and applied a regional Gaussian filter (Swenson et al., 2003) for EL. As described in Swenson et al. (2003), it should be noted that the regional Gaussian filter is not applied to detect the spatial pattern of mass change, but to estimate the amplitude of mass change within a restricted area by taking into account both signal degradation and the leakage effect. The scaling factor of the designed filter was determined following Velicogna et al. (2005); that is, the filter was scaled such that it returned a value of 1 cm when applied to a uniform mass change of 1 cm with water thickness equivalent over the test area. In estimating the leakage effect outside the area of concern, we employed Gaussian-filtered GRACE data, as discussed by Yamamoto et al. (2007). We estimated the approximate magnitude of the leakage correction error from the regional mass estimation using landwater model data for the test. The error is within 4% of total mass variations. In the present study, a 4% error at each point data results in about $\pm 1.5$ mm/yr mass trend error in water thickness equivalent.

We adopted 500 km as the correlation length of the filter. We initially tested several different correlation lengths, ranging from 200 to 1000 km, to evaluate the effect of correlation length on the final result. The maximum difference in interannual mass trend associated with varying correlation length is $\pm 2.1$ mm/yr. This value is smaller than the estimated satellite measurement errors, and has only a minor effect on trend estimation.

### 2.2. ICESat data and processing

GLAS/ICESat L2 Antarctic and Greenland Ice Sheet Altimetry Data (GLA12) Release 28 are currently available for several time periods between 2003 and 2007 (Zwally et al., 2007). To ensure accurate estimates of secular changes, we used 10 datasets of the same repeat orbits for the following periods: 4 October to 18 November 2003, 17 February to 20 March 2004, 3 October to 8 November 2004, 17 February to 23 March 2005, 20 May to 22 June 2005, 21 October to 23 November 2005, 22 February to 27 March 2006, 24 May to 25 June 2006, 25 October to 27 November 2006, and 12 March to 14 April 2007. Saturation elevation correction was applied to the elevation estimates using the correction values included in GLA12 Release 28. Referring to Nguyen and Herring (2005), we used 1) data with gain less than 14, and 2) data with gain of 14–100 and energy below 13.1 fJ. Data with gain >100 were excluded. First, we simply calculated the elevation changes with respect to the digital elevation model (DEM) contained in GLA12 ($30'' \times 30''$ grid). Because the resolution and/or precision of the DEM data are insufficient to accurately recover elevation change, especially in areas with high topographic gradients, we then applied the following process to minimize the effects of DEM errors: 1) select the data along reference ground tracks common to all 10 periods, 2) calculate the average values in small grids ($0.001^\circ \times 0.001^\circ$) for each time period, and 3) calculate elevation changes for the grids between successive periods. In this process, we excluded those data with estimated elevation changes greater than 2 m/yr. Finally, we calculated the average trends on $1^\circ \times 1^\circ$ grids using the small grid data of elevation change for comparison.

### 2.3. Snow-stake measurement data

Measurements of snow accumulation using snow stakes have been conducted at irregular intervals along JARE traverse routes in EL for more than 30 years (National Institute of Polar Research, 1997). In recent years, repeated measurements have been performed between Syowa Station (69°0'S, 39°35'E) and Dome Fuji Station (77°19'S, 39°42E) at intervals of 0.5–5 km. Satow et al. (1999) undertook a detailed analysis of the spatial distribution of snow accumulation and snow density along the traverse route. In the present study, we analyze snow mass accumulation data calculated from snow-stake data and snow density data collected along the route.

### 2.4. PGR mass trend predicted using ice models

Nakada et al. (2000) calculated the rates of gravity change ($\mathrm{d}g/\mathrm{d}t$) and vertical crustal movement ($\mathrm{d}h/\mathrm{d}t$) due to PGR, and provided values at the solid surface of the Earth for seven ice models: ARC3 + ANT4, ARC3 + ANT3, ICE-3 G, ARC3 + HB, ARC3 + D91, ARC3 + ANT5, and ARC3 + ANT6. $\mathrm{d}g/\mathrm{d}t$ depends on both the mass redistribution within the Earth and the height change of the observation point, while GRACE

detects the mass redistribution only. Therefore, the surface density changes detected by GRACE ($d\sigma/dt$) can be approximated by the following equation:

$$\frac{d\sigma}{dt} = \frac{1}{2\pi G}\left(\frac{dg}{dt} - \beta\frac{dh}{dt}\right), \quad (1)$$

where $G$ is the gravitational constant and $\beta = -0.3086$ (μGal/mm) is the free-air gradient. Using Eq. (1), PGR mass trends of the seven ice models were calculated from values of $dg/dt$ and $dh/dt$.

## 3. Results

We first divided the area in EL that shows a mass trend into two basins: Areas A and B in Fig. 1(b). The boundaries given in Fig. 1(b) follow Davis et al. (2005). We also estimated the mass variation for the combined Area A + B. Fig. 2(a)–(c) shows the estimated temporal variations in mass for the Areas A, B and A + B, respectively. Table 1 summarizes the mass trends estimated from the three GRACE datasets released by the different data centers. Note that the errors for GRACE data shown in Fig. 2(a)–(c) are estimated based solely on calibrated standard deviations released by GRACE data centers. In contrast, the errors listed in Table 1 take into account the leakage correction error and erroneous choices of correlation length in the filter design, in addition to the error shown in Fig. 2. Table 2 lists the mass trends estimated from PGR and ice-sheet mass balance. Although pronounced GRACE mass trends were commonly observed in areas A, B, and A + B for the three datasets, they cannot be explained in terms of PGR or ice-sheet mass balance (see Tables 1 and 2). The mass trend in EL is discussed in detail in the following section.

## 4. Discussion

### 4.1. GRACE mass trend and PGR models

In Section 3, we divided the EL area into two basins. One reason for this division is to compare our results with previous mass balance estimations, which also generally divide the EL area into the same two areas (see Table 2). A second reason is to assess whether the mass variations over areas A and B are similar. JARE snow-stake measurement data are only available for Area A; therefore, if the mass variation pattern over Area A differs from that over Area B, it would be inappropriate to use the snow-stake data in explaining snow accumulation over the combined Area A + B. In such a case, we would have to separately discuss the sources of mass variations over areas A and B. As shown in Fig. 2(a)–(c), similar mass variations are observed over areas A, B, and A + B. Thus, we used the snow-stake data in discussing the mass trend over the entire EL area. Although Fig. 2(a)–(c) shows similar temporal variations, it is clear that the errors in Fig. 2(a) and (b) are larger than those in Fig. 2(c). These errors mainly reflect errors in short-wavelength satellite measurements. Fig. 2(c) appears to show the

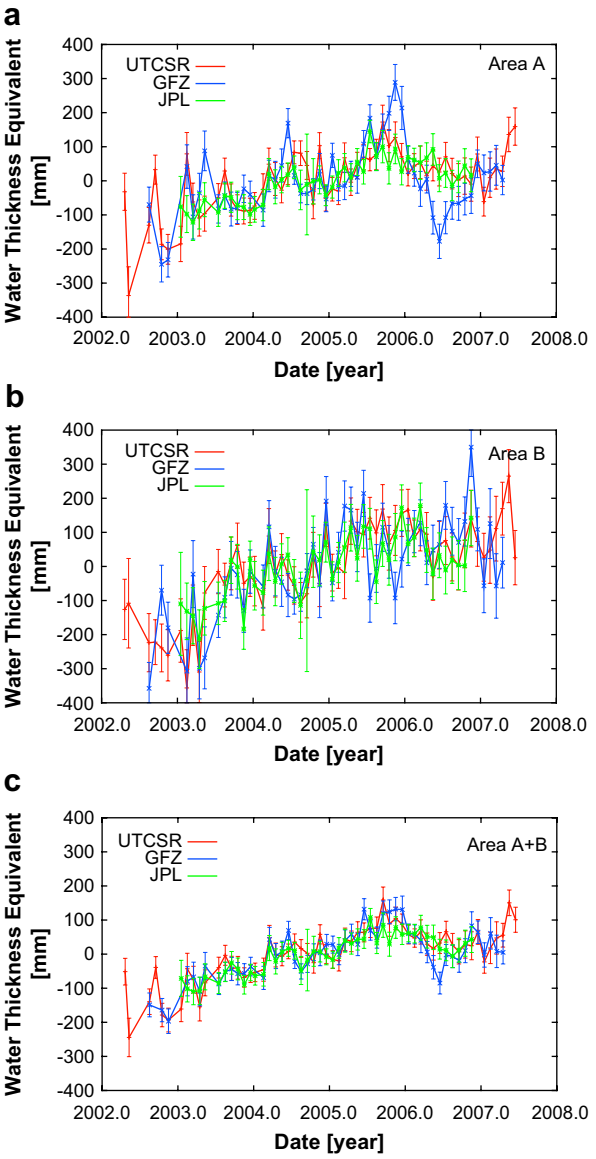


Fig. 2. Estimated GRACE regional mass trends in Enderby Land for Area A (a), Area B (b), and Area A + B (c). GRACE datasets are from Center for Space Research, University of Texas (UTCSR), GeoForshungsZentrum (GFZ) and Jet Propulsion Laboratory (JPL).

Table 1
Interannual mass trend in Enderby Land estimated from GRACE monthly gravity-field solutions based on data from Center for Space Research, University of Texas (UTCSR), GeoForshungsZentrum (GFZ) and Jet Propulsion Laboratory (JPL). $C_{20}$ values are replaced by Satellite Laser Ranging (SLR) solutions. The unit is mm/yr in water thickness equivalent.

| Drainage area ($km^2$) | A ($5.90 \times 10^5$) | B ($3.63 \times 10^5$) | A + B ($9.53 \times 10^5$) |
|---|---|---|---|
| UTCSR | 32.5±8.4 | 61.6±9.6 | 37.4±6.6 |
| GFZ | 19.0±11.8 | 61.6±12.7 | 31.1±8.3 |
| JPL | 41.1±8.0 | 48.6±11.1 | 37.8±6.7 |

most reliable data; therefore, we only refer to Fig. 2(c) in further discussions.

Continuous GPS observations are useful in confirming the accuracy of PGR prediction models. There are two IGS (International GNSS Service) stations in EL: Syowa (SYOG, 69.0070°S, 39.5837°E, located in Area A) and Mawson (MAW1, 67.6048°S, 62.8707°E, located in Area B). Based on analyses of these GPS data, Ohzono et al. (2006) reported vertical uplift values ($dh/dt$ in Eq. (1)) over the period 1998–2004 of $1.37 \pm 0.21$ and $1.29 \pm 0.13$ mm/yr for SYOG and MAW1, respectively. These results are consistent with the small vertical velocities (about 1–4 mm/yr) predicted by several PGR models (Nakada et al., 2000), and indicate the validity of PGR estimates for these areas.

Table 2
Estimated mass trends of post-glacial rebound (PGR) and ice-sheet mass balances. The PGR estimates show the maximum, minimum, and average for the seven ice models reported in Nakada et al. (2000). The unit is mm/yr in water thickness equivalent.

| Drainage area | | A | B | A + B |
|---|---|---|---|---|
| PGR (model) | Maximum | 7.8 | 20 | 11.2 |
| | Minimum | −15 | −5.1 | −11.1 |
| | Average | 2.5 | 7.5 | 4.4 |
| Ice sheet mass balance | | | | |
| Rignot and Thomas (2002) [a] 1992–1997 | | 6.7±0.4 | – | – |
| Zwally et al. (2005) [b] 1992–2002 (grounded + floating) | | −4.6±5.2 | −56.4±11.8 | −17.7±6.8 |

[a] Ice sheet mass balance was given over the Shirase and Rayner glaciers, both of which are located in area A. The mass balance of area A was estimated by dividing the sum of the ice-sheet mass change of the two glaciers ($km^3$/yr, in water equivalent thickness) by the total area of the Shirase and Rayner glaciers. Although the error was assumed to 5%, this value was probably underestimated, as stated by the authors.

[b] The areas of Enderby Land and Kemp Land correspond to areas A and B in the present study, respectively. We summed the mass balances of grounded and floating ice, and divided by the corresponding areas.

### 4.2. Comparison of spatial patterns of GRACE mass trends derived from snow-stake and ICESat data

As stated above, *in situ* snow-stake data are available for the JARE traverse route in Area A. Fig. 3(a) shows the mass trends estimated from the snow-stake data, as well as the snow densities used for height-to-mass conversion. Spatial variations in the trends for the period 2003–2005 are shown in Fig. 3(b). Note that the trend values are averages for 0.5° intervals in latitude. Although the snow density decreases from coastal to inland areas due to decreasing temperature associated with increasing elevation, the variation is too small to explain the surface mass balance. In fact, as shown in Fig. 3(a), the snow density decreases by only 28% from the area with the maximum value (at latitudes 70.0–70.5°S) to the area with the minimum value (at latitudes 77.0–77.3°S), whereas snow mass decreases by 82% (from 20.2 to 3.5 mm/yr; average of the 2003–2005 trend). Thus, the mass decrease from inland to coastal areas cannot be explained solely in terms of increasing snow density; in fact, snow accumulation varies spatially along the route. The spatial pattern of the large mass trend appears to be in good agreement with the GRACE mass trend, especially in coastal areas.

The interannual mass trends and their spatial distribution along the JARE traverse route have been studied in detail by many researchers (National Institute of Polar Research, 1997). The trend of increasing snow accumulation toward the coastal area has existed for at least the past 10 years. This trend mainly reflects the influence of water vapor from the ocean; consequently, the coastal area represents an accumulation zone.

On the slope of the ice sheet in Antarctica, katabatic winds (representing the downward movement of cold air masses under gravity) generate drifting snow throughout the year, meaning that only minor snow accumulation occurs in areas subject to strong katabatic winds of this type. This is the main reason for the small surface mass trend observed around 70°S in Fig. 3(a) and (b). Such spatial patterns mainly depend on the distance from the coastline and topography (elevation and degree of undulation); however, the katabatic wind zone is not clearly defined when Gaussian filters with a correlation length of >200 km are applied to the data, as shown in Fig. 3(c). Similarly, the zone is unclear in the 500 km Gaussian-filtered GRACE mass trend (Fig. 1(b)). Note that the filter used in Fig. 3(c) is normalized only over the traverse route because of the 1-dimensional data distribution, while

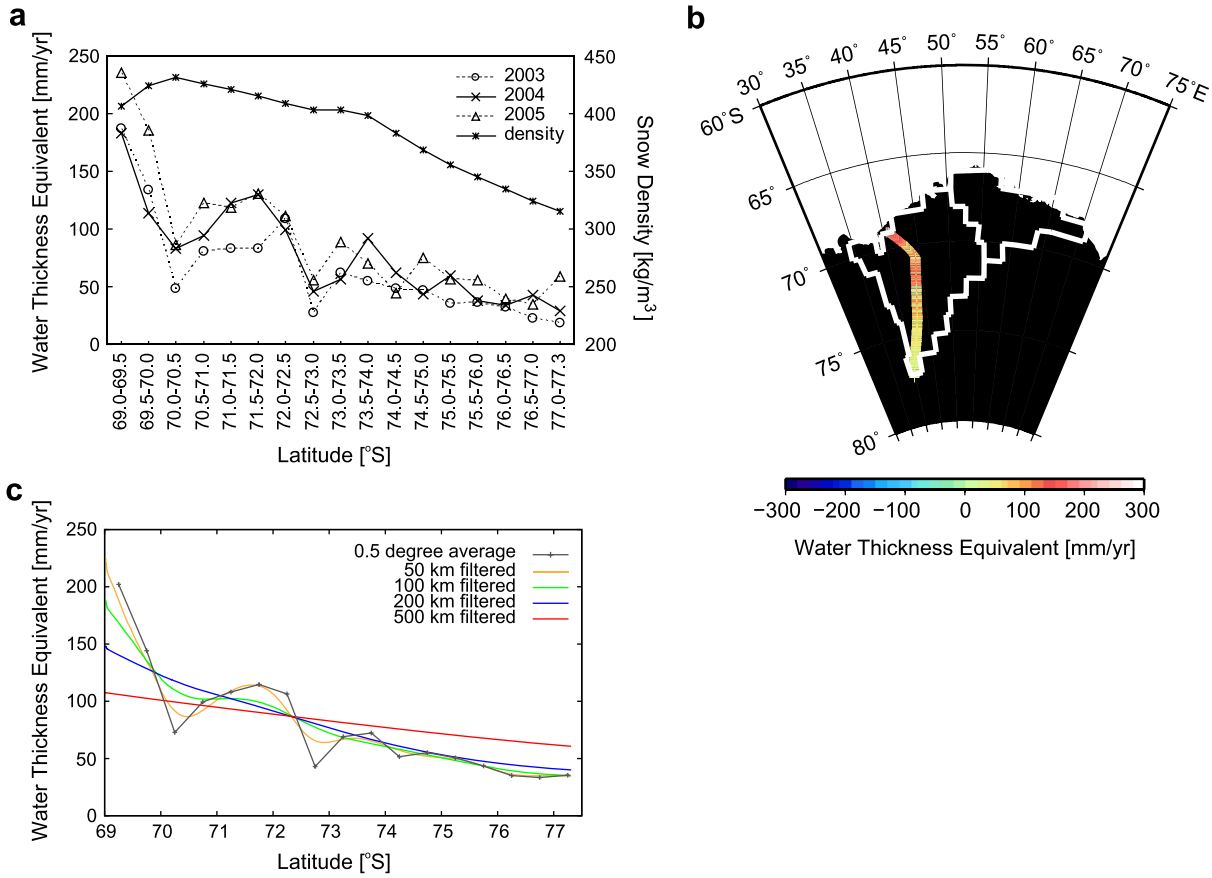


Fig. 3. Interannual surface mass trends estimated based on snow-stake data. (a) Interannual surface mass trend for the period 2003–2005. Snow densities along the traverse route are also plotted. (b) Spatial variations in the interannual surface mass trend for the period 2003–2005. (c) Spatial variations in the 2003–2005 average of the interannual surface mass trend and filtered solutions with correlation lengths of 50, 100, 200, and 500 km. These filters are normalized over the traverse route, but not normalized globally.

a globally normalized filter is used in Fig. 1(b). This difference in normalization gives rise to discrepancies in the spatial patterns and signal magnitude. The spatial pattern in Fig. 1(b) includes a leakage effect from the surrounding area with a small mass trend (i.e., ocean); in contrast, this effect is not taken into account in Fig. 3(c). Thus, the globally normalized filtered GRACE mass trend in Fig. 1(b) shows a maximum at an area located slightly inland from the coast, whereas the snow-stake mass trend in Fig. 3(c) shows a maximum in the coastal area. The magnitude of the trend is discussed in Section 4.3 by comparing the area averages of each dataset.

Fig. 4(a) shows temporal trends in elevation change from 2003 to 2005, as estimated from ICESat data. This period corresponds to that shown in Fig. 3(b). The spatial pattern shows positive elevation trends near the coastal area, consistent with the snow-stake and GRACE data. For comparison with the GRACE trends, Fig. 4(b) shows the ICESat mass trend using the same Gaussian filter as that employed in Fig. 1(b); the two figures show similar spatial patterns. We obtained a correlation coefficient of 0.78 for the 2-dimensional spatial patterns over Area A + B (2003–2005) for GRACE mass trend and ICESat elevation trend. The magnitude of the trend is discussed in Section 4.3, as well as the snow-stake mass trend.

### 4.3. Comparison of time series of GRACE mass variations with snow-stake and ICESat data

Fig. 5 shows the estimated mass variations over the combined Area A + B, based on snow-stake measurements, ICESat, and GRACE data (5-month moving average). ICESat elevation change was converted to mass change based on the average snow density along the traverse route (386 kg/m$^3$) of the snow-stake measurements.

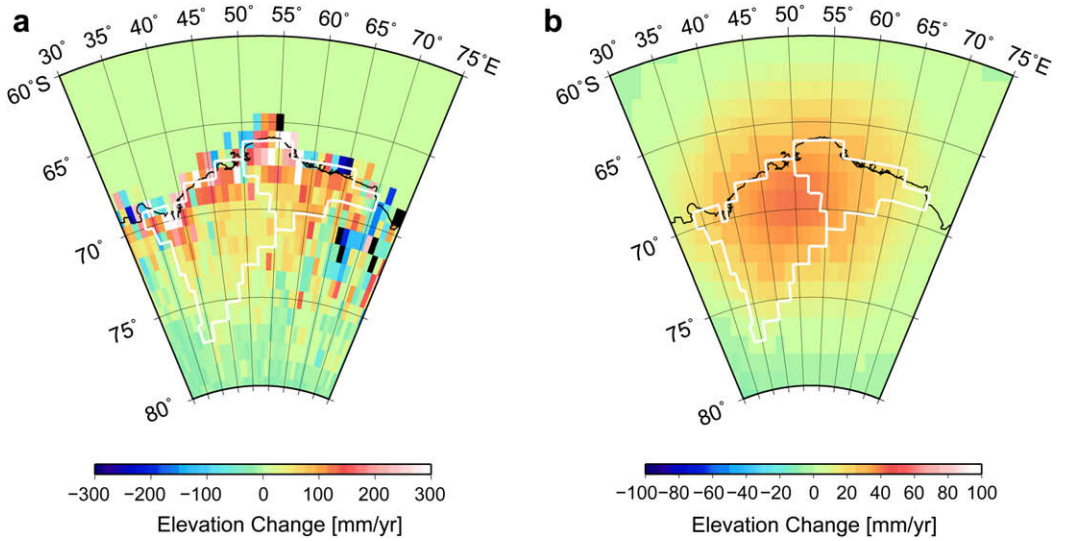


Fig. 4. Elevation change for the period 2003–2005, as estimated based on ICESat data. (a) Non-filtered solution, and (b) globally normalized 500 km Gaussian-filtered solution.

In undertaking snow-stake measurements, snow stakes move horizontally under the influence of snow outflow, leading to positioning errors; however, such movements are negligible in the study of large-scale area. The mass trend in this case is the average over an area of several hundred kilometers. Thus, we regard that the snow-stake data represent the average of 'true' snow accumulation along the traverse route. Although the snow-stake data only cover the traverse route along a coastal–inland transect, the spatial pattern of the mass balance essentially depends on the distance from the coastline – we assumed that longitudinal variations are minor over the study area. Accordingly, we averaged the trend over the traverse route for each time period, and regard this as the snow accumulation over EL.

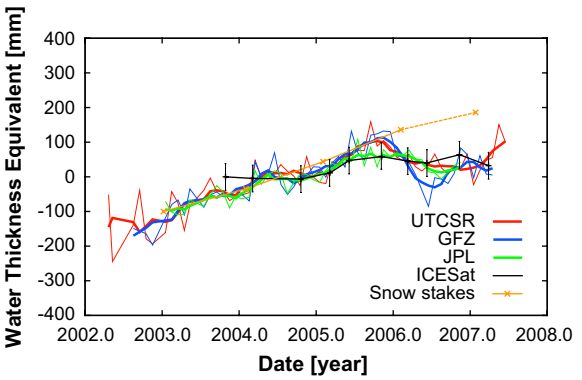


Fig. 5. Time series of GRACE, Ice Cloud and Elevation Satellite (ICESat), and snow-stake mass variation. The GRACE datasets from Center for Space Research, University of Texas (UTCSR), GeoForshungsZentrum (GFZ) and Jet Propulsion Laboratory (JPL) are 5-point moving averages. The most recent snow-stake data (for 2007) were kindly provided by Motoyama, H., National Institute of Polar Research (unpublished data).

For the current release of ICESat data, it is reported that the uncertainty in elevation measurements for each laser shot is about 100 mm, as estimated from the standard deviation at each crossover point (National Snow and Ice Data Center, 2007). The ICESat errors shown in Fig. 5 were calculated by multiplying snow density by a thickness of 100 mm; thus, the estimated error value (in water thickness equivalent) is about 38.6 mm.

Table 3 lists the estimated ICESat, snow stake, and GRACE mass trend values for the period of temporal overlap for the three datasets (from the end of 2003 to the beginning of 2007). As shown in Fig. 5 and Table 3, all three datasets show positive mass trends from 2003 to the middle of 2005. Subsequent to the end of 2005, however, the GRACE and ICESat trends are negative, although the snow-stake trend remains positive. In contrast to the ICESat and GRACE time series, the snow-stake time series increases monotonically. This discrepancy among the different series can possibly be interpreted in terms of basal ice-sheet outflow. The snow-stake measurements observe the sum of snow accumulation, evapotranspiration, and sublimation at the surface, but do not include inflow or outflow of the basal ice sheet. Hence, the snow-stake values are expected to overestimate the true ice-sheet mass balance. In contrast, ICESat observes the total

surface-elevation change, including basal ice-sheet outflow. Thus, it is possible to explain the difference between the snow-stake and ICESat time series (for the period after the end of 2005) in terms of basal ice-sheet flow. In fact, a significant reduction in basal ice-sheet elevation has previously been reported over Area A (Naruse, 1978; Nishio et al., 1989), and has subsequently been confirmed by recent GPS observations.

Table 3 shows that the magnitude of the snow-stake mass trend exceeds the GRACE and ICESat mass trends, even for the period 2003–2005; however, the difference is slight compared with that after the end of 2005. Considering the errors in the ICESat and GRACE mass trends, it is unclear whether the differences for the period 2003–2005 are significant.

Given that the GRACE and ICESat data show a change to negative mass trends from the end of 2005 (Table 3), we tested whether these changes are statistically significant over a long-term trend. We calculated the Akaike's Information Criterion (AIC, Akaike, 1973) value according to the following equation:

$$\mathrm{AIC} = -2\left(\frac{1}{\sqrt{2\pi\sigma^2}}\sum_{i=1}^{N}\left(x_{\mathrm{obs}}^{(i)} - x_{\mathrm{calc}}^{(i)}\right)^2 - \frac{N}{2}\ln 2\pi\sigma^2 - k\right) \quad (2)$$

where $N$ is the number of observed data, $\sigma$ is the standard deviation of the fitting, $x_{\mathrm{obs}}^{(i)} - x_{\mathrm{calc}}^{(i)}$ is the difference between the observed and calculated mass value at the time point $i$, and $k$ is the number of parameters used for fitting. A better fit yields a smaller AIC value. Using the datasets for the period of temporal overlap (from the end of 2003 to the beginning of 2007), we fitted the GRACE and ICESat time series using 1) a monotonically increasing linear function throughout the entire time period (Case 1), and 2) a function that first shows a linear increase, followed by a decrease from the end of 2005 (Case 2); we then compared the resulting AIC values (see Table 4). For both the GRACE and the ICESat time series, Case 1 yielded a smaller AIC value. Thus, at least for the fitting of a long-term GRACE and ICESat mass trend, the linearly increasing function is preferable when taking into account the error levels of current datasets, although the negative trends are obtained as estimated values from the end of 2005 (see Table 3).

Finally, we estimated the PGR mass trend based on GRACE and ICESat data, and validated the accuracy of current ice models (see Table 2). Although the current release of GRACE and ICESat data include large errors, the PGR trend can be derived, in principle, by subtracting the ICESat mass trend from the GRACE trend (Velicogna and Wahr, 2002). If the estimated PGR mass trend would be consistent with the model estimations listed in Table 2, this would also support our results; i.e., the discrepancy between the GRACE trend and the previously reported mass trends listed in Table 2 are mainly caused by small surface-mass changes in the previous reports rather than mismodeling of PGR. Based on a comparison of AIC values, we used the GRACE and ICESat linear mass trends from the end of 2003 to the beginning of 2007 (see Table 3) in estimating the PGR mass trend. The PGR trends estimated from the differences between the GRACE and ICESat mass trends are 10.8 mm/yr in water thickness equivalent for UTCSR, 0.7 mm/yr for GFZ, and 12.2 mm/yr for the JPL GRACE solution. Although the current estimation of PGR mass trend from GRACE and ICESat data has relatively large errors, all of the obtained results are within the uncertainty of several current ice models (see Table 2). Thus, our results demonstrate that the discrepancy between the GRACE data and the sum of previous surface and PGR mass trends reflects the small value of the surface ice-sheet mass trend in Table 2, rather than PGR modeling error.

Table 3
Mass trends estimated for Enderby Land for the periods from September 2003 to October 2005, October 2005 to November 2006, and September 2003 to November 2006, based on snow-stake data, Ice Cloud and Elevation Satellite (ICESat) data, and GRACE datasets from Center for Space Research, University of Texas (UTCSR), GeoForshungsZentrum (GFZ) and Jet Propulsion Laboratory (JPL).

| Time period | Sep 2003–Oct 2005 | Oct 2005–Nov 2006 | Sep 2003–Nov 2006 |
|---|---|---|---|
| Snow stakes | 76.6 | 51.5 | 73.4 |
| ICESat | 30.5±10.0 | −9.5±12 | 18.2±5.3 |
| GRACE (UTCSR) | 68.1±10.4 | −68.0±32.4 | 29.1±5.6 |
| GRACE (GFZ) | 72.4±11.0 | −72.3±33.0 | 19.0±5.7 |
| GRACE (JPL) | 61.0±9.9 | −60.9±30.9 | 30.4±5.5 |

Table 4
Akaike's Information Criterion (AIC) values estimated by two types of fitting for Ice Cloud and Elevation Satellite (ICESat) time series and GRACE time series from Center for Space Research, University of Texas (UTCSR), GeoForshungsZentrum (GFZ) and Jet Propulsion Laboratory (JPL) for the period September 2003 to November 2006. Case 1 involved a monotonically increasing linear function throughout the entire period. Case 2 involved a function with an initial linear increase, followed by a decrease from the end of 2005.

| AIC | Case 1 | Case 2 |
|---|---|---|
| ICESat | −27.9 | −18.6 |
| GRACE (UTCSR) | −578.0 | −155.9 |
| GRACE (GFZ) | −910.8 | −418.4 |
| GRACE (JPL) | −423.1 | −63.2 |

## 5. Conclusions

In this study, we compared the GRACE mass trend with snow-stake data and ICESat data in Enderby Land (EL), Antarctica. The spatial patterns of the mass trends show good agreement with each other. In contrast, the time series of snow-stake mass variations averaged over EL diverges from the GRACE time series after the end of 2005; the ICESat and GRACE trends are similar. The discrepancy between snow-stake and GRACE data probably reflects the influence of basal ice-sheet flow. Based on a comparison among current PGR models and the estimated PGR mass trend from GRACE and ICESat, we concluded that the discrepancy between the GRACE data and previous reports of ice-sheet mass balance and PGR models can be explained by the small values of surface ice-sheet mass change described in previous reports. Although both GRACE and ICESat data are lacking in accuracy when evaluating the PGR trend, improved and longer-period datasets should enable us to evaluate the PGR trend with greater accuracy in the future. *In situ* observations, such as GPS and snow-stake measurements, are expected to play an important future role in the interpretation of satellite data, as shown in this study.

## Acknowledgments

This research was conducted as part of the project ''Calibration/Validation of GRACE-Derived Gravity Fields Using the Ground Data Obtained in the Japanese Antarctic Research Expedition area and Syowa Station, Antarctica'' approved for NRA-01-OES-05 (principal investigator, Kazuo Shibuya).

## References

Akaike, H., 1973. Information theory and an extension of maximum likelihood principle. In: Petrov, B.N., Csaki, F. (Eds.), Second International Symposium on Information Theory. Akademial Kaido, Budapest, pp. 267–281.

Bettadpur, S., 2007. UTCSR Level-2 Processing Standards Document for Level-2 Product Release 0004, GRACE 327–742 (CSR-GR-03-03). Center for Space Research, the University of Texas at Austin, Austin.

Cheng, M., Ries, J., 2007. GRACE Technical Note #05: Monthly Estimates of C20 From 5 SLR Satellites Available from: http://podaac.jpl.nasa.gov/grace/documentation.html#5.

Chen, J.L., Wilson, C.R., Blankenship, D.D., Tapley, B.D., 2006. Antarctic mass rates from GRACE. Geophys. Res. Lett. 33 (L11502), doi:10.1029/2006GL026369.

Davis, C.H., Ki, Y., McConnell, J.R., Frey, M.M., Hanna, E., 2005. Snowfall-driven growth in East Antarctic ice sheet mitigates recent sea-level rise. Science 308, 1898–1901.

Flechtner, F., 2007. GFZ Level-2 Processing Standards Document for Level-2 Product Release 0004, GRACE 327–743 (GR-GFZ-STD-001). GeoForschungszentrium, Potsdam, Wessling.

Church, J.A., Gregory, J.M., Huybrechts, P., Kuhn, M., Lambeck, K., Nhuan, M.T., Qin, D., Woodworth, P.L., 2001. Changes in sea level. In: Houghton, J.T. (Ed.), Climate Change 2001: the Scientific Basis. Contribution of Working Group I to the Third Assessment Report of the Intergovernmental Panel on Climate Change. Cambridge University Press, Cambridge, pp. 639–694.

Ivins, E., James, T.S., 2005. Antarctic glaciological isostatic adjustment: a new assessment. Antarct. Sci. 17, 541–553, doi:10.1017/S0954102005002968.

Nakada, M., Kimura, R., Okuno, J., Moriwaki, K., Miura, H., Maemoku, H., 2000. Late Pleistocene and Holocene melting history of the Antarctic ice sheet derived from sea-level variations. Mar. Geol. 167, 85–103.

Naruse, R., 1978. Surface flow and strain of the ice sheet measured by a triangulation chain in Mizuho Plateau. Mem. Natl. Inst. Polar Res., 198–226 (Special issue 7).

National Institute of Polar Research, 1997. Antarctica: East Queen Maud Land – Enderby Land Glaciological Folio. Folio. National Institute of Polar Research, Tokyo, ISBN 4-906651-00-3.

National Snow and Ice data Center, 2007. Available from: http://nsidc.org/data/icesat/detailed_disclaimer.html.

Nguyen, A.T., Herring, T.A., 2005. Analysis of ICESat data using Kalman filter and kriging to study height changes in Antarctica. Geophys. Res. Lett. 32 (L23S03), doi:10.1029/2005GL024272.

Nishio, F., Mae, S., Ohmae, H., Takahashi, S., Nakawo, M., Kawada, K., 1989. Dynamic behaviour of the ice sheet in Mizuho Plateau, East Antarctica. Proc. NIPR Symp. Polar Meteorol. Glaciol. 2, 97–104.

Ohzono, M., Tabei, T., Doi, K., Shibuya, K., Sagiya, T., 2006. Crustal movement of Antarctica and Syowa Station based on GPS measurements. Earth Planets Space 58, 795–804.

Peltier, W.R., 2004. Global glacial isostasy and the surface of the ice-age earth: the ICE-5G (VM2) model and GRACE. Ann. Rev. Earth Planet. Sci. 32, 111–149, doi:10.1146/annurev.earth.32.082503.144359.

Rignot, E., Thomas, R.H., 2002. Mass balance of polar ice sheets. Science 297 (5586), 1502–1506, doi:10.1126/science.1073888.

Satow, K., Watanabe, O., Shoji, H., Motoyama, H., 1999. The relationship among accumulation rate, stable isotope ratio and surface temperature on the plateau of east Dronning Maud Land, Antarctica. Polar Meteorol. Glaciol. 13, 43–52.

Swenson, S., Wahr, J., Milly, P.C.D., 2003. Estimated accuracies of regional water storage variations inferred from the Gravity Recovery and Climate Experiment (GRACE). Water Resour. Res. 39, 1223, doi:10.1029/2002WR001808.

Tapley, B.D., Bettadpur, S., Watkins, M., Reigber, C., 2004. The gravity recovery and climate experiment: mission overview and early results. Geophys. Res. Lett. 31 (L09607), doi:10.1029/2004GL019920.

Velicogna, I., Wahr, J., 2002. A method for separating Antarctic postglacial rebound and ice mass balance using future ICESat Geoscience Laser Altimeter System, Gravity Recovery and Climate Experiment, and GPS satellite data. J. Geophys. Res. 107 (B10) 2263, doi:10.1029/2001JB000708.

Velicogna, I., Wahr, J., Hanna, E., Huybrechts, P., 2005. Short term mass variability in Greenland, from GRACE. Geophys. Res. Lett. 32 (L05501), doi:10.1029/2004GL021948.

Velicogna, I., Wahr, J., 2006. Measurements of time-variable gravity show mass loss in Antarctica. Science 311, 1754–1756, doi:10.1126/science.11237785.

Wahr, J., Molenaar, M., Bryan, F., 1998. Time variability of the Earth's gravity field: hydrological and oceanic effects and their possible detection using GRACE. J. Geophys. Res. 103 (B12), 30205–30229, doi:10.1029/98JB02844.

Watkins, M.M., 2007. JPL Level-2 Processing Standards Document for Level-2 Product Release 04, GRACE 327–744. Jet Propulsion Laboratory, Pasadena.

Yamamoto, K., Fukuda, Y., Nakaegawa, T., Nishijima, J., 2007. Landwater variation in four major river basins of the Indochina peninsula as revealed by GRACE. Earth Planets Space 59, 193.

Zwally, H.J., et al., 2002. ICESat's laser measurements of polar ice, atmosphere, ocean and land. J. Geodyn. 34, 3–4, doi:10.1016/S0264-3707(02)00042-X. 405–445.

Zwally, H.J., Giovanetto, M.B., Li, J., Cornejo, H.G., Beckley, M.A., Brenner, A.C., Saba, J.L., Yi, D., 2005. Mass changes of the Greenland and Antarctic ice sheets and shelves and contributions to sea-level rise: 1992–2002. J. Glaciol. 51, 175.

Zwally, H.J., Schutz, R., Bentley, C., Bufton, J., Harring, T., Minster, J., Spinhirne, J., Thomas, R., 2007. GLAS/ICESat L2 Antarctic and Greenland Ice Sheet Altimetry Data (GLA12) V5.2 (Release 28). National Snow and Ice Data Center, Boulder.